



Published in final edited form as:

J Immunol. 2011 July 1; 187(1): 350–360. doi:10.4049/jimmunol.1004144.

IL-6 mediates the susceptibility of gp130 hypermorphs to *Toxoplasma gondii*

Jonathan S Silver^{*}, Jason S. Stumhofer^{*}, Sara Passos^{*}, Matthias Ernst², and Christopher A. Hunter^{*}

^{*} Department of Pathobiology, School of Veterinary Medicine, Hill Pavilion, 380 S. University Avenue, University of Pennsylvania, Philadelphia PA USA

² Ludwig Institute for Cancer Research, Victoria, Australia

Abstract

IL-6 and IL-27 are closely related cytokines that play critical, but distinct, roles during infection with *Toxoplasma gondii*. Thus, IL-6 is required for the development of protective immunity to this pathogen, while IL-27 is required to limit infection-induced pathology. Paradoxically, these factors both signal through glycoprotein 130 (gp130), but little is known about how the signals downstream of gp130 are integrated to coordinate the immune response to infection. To better understand these events, gp130 Y757F mice that have a mutation in gp130 at the binding site for Suppressor of cytokine signaling 3 (SOCS3), a critical negative regulator of gp130 signaling, were infected with *T. gondii*. These mutant mice were acutely susceptible to this challenge, characterized by an early defect in the production of IL-12 and IFN- γ , and increased parasite burdens. Consistent with the reduced IL-12 levels, IL-6, but not other gp130 cytokines, was a potent antagonist of IL-12 production by gp130 Y757F macrophages and dendritic cells *in vitro*. Moreover, in gp130 Y757F mice, blocking IL-6 *in vivo*, or administration of recombinant IL-12, during infection restored IFN- γ production and protective immunity. Collectively, these studies highlight that a failure to abbreviate IL-6-mediated gp130 signaling results in a profound anti-inflammatory signal that blocks the generation of protective immunity to *T. gondii*.

Introduction

The transmembrane protein gp130 is a signal-transducing component of the receptors used by several closely related cytokines that includes IL-6 and IL-27, as well as IL-11, Oncostatin M, Leukemia Inhibitory Factor, Cardiotrophin-like cytokine, Cytokine-Like Factor 1 and Ciliary Neurotrophic Factor (1). Binding of IL-6/gp130 family members to their specific receptor alpha chains allows for high-affinity interactions with gp130 and activation of Janus Kinases (JAK1, JAK2 and Tyk2), which ultimately results in recruitment of Signal Transducers and Activators of Transcription (STAT) –1 and –3. Following phosphorylation, the STATs dimerize and translocate to the nucleus where they can act as transcription factors. There are several mechanisms in place that limit gp130-mediated Jak/STAT signaling; these include dissociation of JAKs from the receptor, endocytosis of the receptor complex, and nuclear export and dephosphorylation of activated STAT molecules (2). However, members of the Suppressor of Cytokine Signaling (SOCS) family are regarded as the most prominent regulators of STAT signaling. These proteins are induced in response to several cytokines that utilize the STAT-signaling pathway and, among the SOCS family members, SOCS3 plays a critical role in specifically limiting gp130-mediated signaling. This inhibitory effect has been associated with the ability of SOCS3 to bind to

^{*}Correspondence should be addressed to: CA Hunter (chunter@vet.upenn.edu).

gp130 at the tyrosine residue in position 757, as well as its ability to act as a ubiquitin ligase, targeting the associated receptor complex for degradation (3–7).

The significance of SOCS3 in limiting gp130 signaling is illustrated by the work of two groups that generated gp130 mutant mice: gp130 Y757F mice have a mutation in the binding site of SOCS3, while gp130 Y759F mice express the human gp130 receptor with a similar mutation (8, 9). In both cases, activation of STAT3 is sustained in response to stimulation with gp130-signaling cytokines, which leads to aberrant pathology. For example, the gp130 Y757F mice develop gastric adenoma, hematopoietic defects, driven by IL-11 and IL-6, respectively (10, 10–13). In contrast, gp130 Y759F mice develop an autoimmune arthritis driven by STAT3-mediated overproduction of IL-7 (14, 15). Consistent with the phenotype of the gp130 mutant mice, multiple studies have highlighted the role of this receptor and its corresponding cytokines in mediating the inflammation associated with cancer and autoimmunity (16–18). However, despite the body of work highlighting the importance of regulated gp130-mediated signaling in inflammation associated with cancer and autoimmunity, very little is understood about how control of gp130-mediated signaling impacts infection-induced inflammation.

T. gondii is an obligate intracellular parasite that is an important opportunistic infection in immunocompromised individuals, especially those with defects in T cell function (19, 20). Challenge with this organism induces a highly polarized Th1 response characterized by production of IL-12 by macrophages, neutrophils and dendritic cells, which leads to IFN- γ production by NK cells, as well as CD4⁺ and CD8⁺ T cells (21, 22). IFN- γ is the major mediator of resistance to *T. gondii* and induces a variety of anti-microbial mechanisms that allow the host to control this infection (23). Relevant to this work, the cytokines IL-6 and IL-27, which both signal through gp130, have important roles during experimental toxoplasmosis. Thus, mice deficient in IL-6 develop high cyst burdens and succumb to a severe encephalitis associated with a failure to control parasite replication (24, 25). In addition, mice that lack gp130 specifically in astrocytes are more susceptible to infection due to uncontrolled parasite replication, resulting in pathology in the brain (26). Thus, IL-6 and gp130 are essential for the development of a protective immune response that allows the host to control parasite replication. In contrast, mice that lack WSX-1, the alpha chain of the IL-27 receptor, control this parasite effectively but develop lethal T cell-mediated immunopathology, indicating that IL-27 plays a critical role in limiting infection-induced inflammation and pathology (27, 28). Together, these studies highlight the diverse signals through gp130 that are required to coordinate a balanced immune response that allows the host to control *T. gondii* while limiting the development of immune pathology. These findings are also relevant to other infectious models, where IL-6 and IL-27 contribute to the control of pathogen replication or limit pathology, respectively (29). However, little is known about the factors that coordinate the balance between the pro- and anti-inflammatory signals of gp130 during infection.

In order to better understand how gp130-mediated signaling coordinates the immune response against a pathogen, gp130 Y757F mice were infected with *T. gondii*. Unlike WT littermate controls, mutant mice succumbed to this challenge due to an inability to control parasite replication. Susceptibility was associated with defective production of IL-12 and IFN- γ by dendritic and NK cells, respectively, which correlated with the ability of IL-6 to block the production of IL-12 by gp130 Y757F dendritic cells and macrophages. Accordingly, administration of IL-6 blocking antibodies or recombinant IL-12p70 during infection restored the production of IFN- γ and decreased parasite burdens in gp130 Y757F mice. Collectively, these studies highlight that a failure to abbreviate IL-6-mediated gp130 signaling results in a profound anti-inflammatory signal that blocks the generation of protective immunity to *T. gondii*.

Materials and Methods

Mice and parasites

Gp130 Y757F mice on a B6 and B6/129 background were provided by Dr. Mathias Ernst (Ludwig Institute, Melbourne Australia), and have been previously described (8). RAG mice are maintained in house. Mice were housed and bred in specific pathogen-free facilities in the Department of Pathobiology at the University of Pennsylvania in accordance with institutional guidelines. The Me49 Strain of *T. gondii* was prepared from chronically infected CBA/ca mice and experimental animals were infected intraperitoneally with 20 cysts. For IL-6 blockade, mice were treated intraperitoneally with 100 μ g of anti IL-6 blocking antibodies (BioXcell, Lebanon, New Hampshire) one day before infection and at days 2 and 5 post-infection. For 250 ng of recombinant murine IL-12p70 (PeproTech, Rocky Hill, NJ) was given intraperitoneally on the day of infection as well as days 1, 2 and 3 post-infection. Soluble toxoplasma antigen (STAg) was prepared from tachyzoites of the RH strain as previously described and used at a concentration of 10 μ g/mL for antigen specific recalls. For histology, livers, lungs and brains were collected from mice, fixed in 10% formalin, embedded in paraffin, sectioned and stained with hematoxylin and eosin. For measurement of parasite burden, the 35-fold repetitive *T. gondii* *B1* gene was amplified by real-time PCR with SYBR Green PCR Master mix (Applied Biosystems, Foster City, California) in an AB7500 fast real-time PCR machine (Applied Biosystems) using previously published conditions (30). To assess parasite burden by cytospin count, single-cell suspensions were prepared from PECs, and 1×10^5 cells in 200 μ l RPMI 1640 were spun onto glass slides at 500 rpm for 5 min. Slides were stained with Diff Quick (Merck, Darmstadt, Germany) and mounted in CytoSeal (Edmund Scientifics, Tonawanda, NY). The percentage of infected cells was calculated based on counts of at least 250 total cells.

Preparation of Bone Marrow-derived macrophages and isolation of primary DC

Bone marrow from naïve WT and gp130 Y757F littermates was harvested and single cell suspensions were cultured at a density of 4×10^5 cells per Petri dish for 7 days. DMEM was supplemented with HEPES, Penicillin, Streptomycin, Sodium Pyruvate and cell-free supernatant from cultures of L929 fibroblasts. Media and L929 supernatant was replenished at day 4.

For isolation of primary dendritic cells, spleens and LN were pooled from 2–3 6–8 week old naïve WT and gp130 Y757F mice. Single cell suspensions were lysed in 0.86% NH_4Cl and run on Lympholyte gradients to enrich for live cells. Remaining cell suspensions were then used to purify CD11c^+ dendritic cells using a MACS column (Miltenyi, Bergisch Gladbach, Germany) according to manufacturer's protocol. 7.5×10^4 purified DCs were cultured per well in 200 μ L of complete RPMI in a 96-well plate and activated with LPS (100ng/ml), $\text{IFN-}\gamma$ (100U/mL), IL-6 (50 ng/ml) or IL-27 (100ng/mL; Amgen, Thousand Oaks, California) for 24 hours before harvesting supernatants for ELISA.

For intracellular cytokine staining, macrophages or DC were stimulated in the presence of media or with LPS (100ng/ml; Sigma Aldrich, Saint Louis, MO), $\text{IFN-}\gamma$ (100U/mL; R&D, Minneapolis, MN), IL-6 (50ng/ml; eBiosciences, San Diego, California) and Brefeldin A for 8–12 hours before being fixed with 4% PFA, permeabilized with 0.5% Saponin in Flow Cytometry buffer and stained intracellularly for IL-12p40 (eBiosciences, San Diego, California).

T cell transfers

For T cell transfers into $\text{RAG}^{-/-}$ mice, spleens and lymph nodes were pooled from 2 to 3 naïve WT or gp130 Y757F mice. Single cell suspensions were lysed with 0.86% NH_4Cl and

run on a Lympholyte (Cedarlane Laboratories Limited, Burlington, Ontario, Canada) gradient to enrich for live cells. The remaining cells were then run over a T cell purification column (R&D, Minneapolis, MN) according to manufacturer's protocol to purify CD3⁺ T cells. 8 to 10 million total CD4⁺ and CD8⁺ T cells were transferred into RAG knockout mice 3 days before being infected ip with *T. gondii*. Mice were sacrificed at day 8 post-infection for analysis of parasite burden and cytokine production.

Intracellular staining for phosphorylated STAT1 and STAT3

CD4⁺ T cells were purified from WT or gp130 Y757F mice with a CD4⁺ isolation kit (Milltenyi). Purified CD4⁺ T cells (1×10^6) were incubated with IL-6 for 5, 30, 60 or 180 min. Cells were then fixed for 10 min at 37 °C with 2% paraformaldehyde. After being fixed, cells were made permeable for 30 min on ice with 90% methanol, then were stained for CD4 and phosphorylated STAT1 and STAT3. *In vitro* differentiation of IL-10 producing CD4⁺ T cells was done as previously described (31).

Flow Cytometry Antibodies

FITC DX5 (Dx5), Alexa Fluor 488 Phospho STAT3 (pS727, clone 49/p-stat3), Alexa Fluor 647 Phospho STAT1 (pY701, clone 4a), PE IL-17 (TC11-18H10), and PerCP Cy5.5 CD4 (RM4-5) were purchased from BD Biosciences (San Jose, CA). FITC anti-MHC II IA/IE (M5/114.15.2), PerCP-Cy5.5 CD11b (M1/70), Pe-Cy7 CD11c (N418), Allophycocyanin CD62L (IM7), Allophycocyanin IFN- γ (XMG1.2), Allophycocyanin IL-10 (JES5 16E3) and Allophycocyanin Alexa Fluor-750 anti CD3 (17A2) were purchased from eBiosciences (San Diego, CA). PE anti-CD126 (IL-6 receptor alpha chain, 255821), Allophycocyanin anti-CD130 (gp130, 125623) were purchased from R&D Systems (Minneapolis, MN). PE-Cy7 CD62L (MEL-14), Pacific Blue anti CD3 (17A2), Pacific Blue anti-CD19 (6D5) and Pacific Blue anti-NK1.1 (PK136) were purchased from BioLegend (San Diego, CA)

Statistical Analysis

An unpaired Student's *t*-test or one-way ANOVA was used to determine significant differences, and *P* values less than 0.05 were considered significant.

Results

Gp130 Y757F mice are susceptible to *T. gondii*

To address the role of gp130-signaling in the regulation of the immune response to infection, gp130 Y757F mice were challenged with the Me49 strain of *T. gondii*. While WT littermate controls survived to the chronic phase of infection, gp130 Y757F mice succumbed by day 12 (Figure 1A). Microscopic analysis of peritoneal exudates cells (PECs) at day 8 post-infection revealed that, as expected, WT mice controlled parasite replication with less than 5% of PECs infected. In contrast, gp130 Y757F mice had more than 35% of peritoneal cells infected at this time point (Figure 1B). Consistent with these data, real-time PCR to quantify parasite DNA at the same time point revealed increased parasite burdens in the liver and brain of gp130 Y757F mice (Figure 1, C and D). This high parasite burden was accompanied by the presence of overt inflammation in multiple peripheral tissues, in particular the lungs (Figure 1, E-H).

Gp130 Y757F mice have an early defect in the ability to produce IL-12

The ability of IL-12 to promote the production of IFN- γ is critical for the control of *T. gondii* and defects in this pathway lead to heightened susceptibility to this infection (21, 22). Therefore, to determine if dysregulated gp130-mediated signaling resulted in alterations in the production of IL-12, a kinetic analysis of the levels of this cytokine was performed. In

uninfected mice, there were low basal amounts of serum IL-12p40 (data not shown), but infection of WT mice resulted in increased circulating levels of this cytokine by days 3 and 8 post-infection (Figure 2A). In contrast, gp130 Y757F mice had significantly lower circulating levels of this cytokine at day 3 post-infection, but by day 8 levels were comparable to WT mice (Figure 2A). These differences in IL-12p40 production were also observed when whole splenocytes from mice infected for three days were stimulated with STAg (Figure 2B), whereas splenocytes from mice infected for eight days produced equivalent levels of IL-12p40 (data not shown). Moreover, analysis of the PECs at day 4 post-infection revealed that, while 4–8% of WT DCs produce IL-12p40 after infection, a smaller percentage of gp130 Y757F DCs stained positive for intracellular IL-12p40, and this difference is reflected in the total number of IL-12p40⁺ DCs (Figure 2C, D). Despite the difference in the number of IL-12⁺ DC, the expression of MHC II (Figure 2E) is not different between DC in WT and Y757F mice. Taken together, these data demonstrate that gp130 Y757F mice infected with *T. gondii* have an early deficiency in the production of IL-12, but this does not correlate with differences in overall activation.

Gp130 Y757F mice have lower levels of IFN- γ early after *T. gondii* infection, despite normal T cell activation

The early production of IL-12 following challenge with *T. gondii* drives the secretion of IFN- γ by NK and T cells, which is required to control this infection (21). In order to determine whether the early defects in IL-12 levels observed in gp130 Y757F mice affected the expression of IFN- γ , a kinetic analysis of this cytokine was performed. In naïve WT and gp130 Y757F mice, there were low basal levels of circulating IFN- γ (data not shown), but by day 3 post-infection, WT mice had ~7ng/mL of IFN- γ circulating in the serum, while gp130 Y757F mice had significantly lower levels of this cytokine (Figure 3A). However, by day 8 post-infection WT and gp130 Y757F mice have equivalent levels of IFN- γ (Figure 3A). Stimulation of whole splenocytes from mice infected for 3 days with STAg mirrored the defect in circulating IFN- γ levels, and cells from WT controls produced significantly more than gp130 Y757F (Figure 3B).

In order to determine the functional consequence of the early defect in IFN- γ production in gp130 Y757F mice, real time PCR was used to quantify the expression of the IFN- γ -inducible p47 GTPases IGTP, Lrg47 and IGIP, which are required for resistance to *T. gondii* (32–34). Relative to the levels in naïve mice, infection of WT mice induced a 10–20 fold increase in expression of IGTP, Lrg47 and IGIP in the livers from WT mice by day 3 post-infection (Figure 3C). In contrast, the levels of these GTPases in gp130 Y757F mice only increased by 1–2 fold (Figure 3C). These data indicate that the gp130 Y757F mice have an early defect in the production of IFN- γ and reduced expression of antimicrobial effector molecules downstream of this cytokine.

Since NK cells are an innate source of IFN- γ and IL-17 during acute toxoplasmosis (35, 36), studies were performed to assess whether the gp130 Y757F NK cells have a defect in the ability to produce this cytokine. WT and gp130 Y757F mice were infected and at day 4 post-infection splenocytes were stimulated *ex vivo* with PMA/Ionomycin and Brefeldin A for four hours before being stained for intracellular IFN- γ and IL-17. As shown in Figure 3D and 3E, gp130 Y757F mice have fewer IFN- γ ⁺ NK cells at this time point, but consistent with the ability of IL-6 to drive the production of IL-17 by NK cells (37), gp130 Y757F mice have significantly more IL-17⁺ NK cells (Figure 3D, F). By day 8 post-challenge, the NK cell response was diminished, and few of these cells produced IFN- γ or IL-17 (data not shown), consistent with reports that the NK cell response to *T. gondii* peaks 4–5 days after infection (37–39).

To assess whether the altered signaling through gp130 also affected the T cell compartment, studies were performed to compare the T cell responses in WT and gp130 Y757F mice. At days 4 and 8 post-infection, there were equivalent percentages and total numbers of activated CD44^{high} CD62L^{low} CD4⁺ T cells in the spleens of infected WT and gp130 Y757F mice (Figure 4A and B) and similar results were observed for CD8⁺ T cells (data not shown). Single cell analysis revealed that there were similar percentages and total numbers of IFN- γ ⁺ CD4⁺ T cells in WT and gp130 Y757F mice at day 4 and day 8 post-challenge (Figure 4C and D). Additionally, stimulation of splenocytes from infected mice with anti-CD3 at day 8 post-infection show equivalent production of IFN- γ between WT and gp130 Y757F mice (Figure 4E). These data suggest that the T cell response is normal in gp130 Y757F mice, and that the diminished early production of IFN- γ is due to an NK cell defect.

Gp130 Y757F T cells produce augmented levels of IL-10 in response to IL-6 and IL-27, but are still protective during toxoplasmosis

One possible explanation for the early defect in IL-12 levels during infection of gp130 Y757F mice is increased expression of IL-10, a potent antagonist of IL-12 production, which can be promoted by IL-6 and IL-27 (31, 40–45). Indeed, experiments assessing the activation and phosphorylation of STAT molecules in response to IL-6 (Figure 5A) and IL-27 (Supplemental Figure 1 and (28)) on T cells revealed that responsiveness to both cytokines was enhanced in gp130 Y757F cells compared to WT cells, as measured by levels of intracellular phospho-STAT3 and STAT1 (data not shown). Additionally, naïve CD4⁺ T cells from gp130 Y757F mice produce significantly higher levels of IL-10 when activated in the presence of TGF- β and IL-6 or IL-27 (Figure 5B). *In vivo*, although IL-10 was not detected in the serum of naïve mice of either genotype (data not shown), by 8 days post-infection serum IL-10 levels in gp130 Y757F mice were almost twice those detected in WT mice (Figure 5C). Moreover, when splenocytes from infected gp130 Y757F mice were re-stimulated *ex vivo* with anti-CD3 there was a significant increase in the production of IL-10 compared to WT cells (Figure 5D). There was also a 2–4 fold increase in the percentage of IL-10⁺ CD4⁺ T cells as revealed by intracellular cytokine staining and this was reflected in the total number of splenic IL-10⁺ CD4⁺ T cells. (Figure 5E and 5F). Thus, the production of the potent anti-inflammatory cytokine IL-10 is augmented in gp130 Y757F mice during toxoplasmosis.

Previous studies demonstrated that CD4⁺ T cells are the primary source of host-protective IL-10 during toxoplasmosis (46). Therefore, in order to determine if the enhanced production of IL-10 by gp130 Y757F T cells contributed to the increased susceptibility to infection, experiments were performed utilizing a RAG transfer system. In these experiments, 10 million CD4⁺ and CD8⁺ T cells isolated from spleens and lymph nodes of naïve WT and gp130 Y757F mice were transferred into RAG 2 KO mice one day prior to infection. At day 8 post-infection, mice were sacrificed and analyzed for parasite burden and cytokine production. While infected RAG2 KO mice have high parasite burdens at this time point, mice that received WT or gp130 Y757F T cells had a significant reduction in the percentage of infected PECs (Figure 5G). Additionally, there were equivalent percentages of IFN- γ ⁺ CD4⁺ T cells in splenocytes of recipient mice (Figure 5H), and the transferred T cells produced equivalent levels of IFN- γ upon *ex vivo* STAg (Figure 5I) and anti-CD3 (data not shown) re-stimulation. Similarly to infected gp130 Y757F mice, transferred gp130 Y757F T cells produced significantly more IL-10 during infection compared to WT T cells (Figure 5J), but these mice were able to appropriately control the infection based on parasite burden in the PECs (Figure 5G). Together, these experiments demonstrate that the over-production of IL-10 is intrinsic to the gp130 Y757F T cells, and can be driven by IL-6 and IL-27, but that this phenotype does not account for the increased susceptibility of the gp130 Y757F mice.

IL-6 blocks the production of IL-12 by gp130 Y757F APC

Taken together, these experiments suggest that the ability of gp130 Y757F T cells to protect during challenge with *T. gondii* is not compromised, and indicate that the susceptibility of gp130 Y757F mice to *T. gondii* is due to an intrinsic defect in the innate immune response. Previous work demonstrated that in the absence of SOCS3, IL-6 acquired the ability to block LPS-mediated IL-12 production by macrophages, providing a potential mechanism underlying the IL-12 defect in gp130 Y757F mice (47–49). In order to assess whether IL-6 could be acting directly on innate APCs during infection, macrophages and DCs in the PECs were analyzed by flow cytometry for the IL-6 receptor alpha chain and gp130 at day 4 post-infection. In both cell types, the expression of gp130 was ubiquitous and all cells expressed this receptor (Figure 6A), while about 50% of each population expressed the IL-6 receptor alpha chain (Figure 6A). There were no differences in the expression of either chain of the receptor between cells from either naïve or infected WT and gp130 Y757F mice. Strikingly, significantly more MHCII positive PEC DCs expressed the IL-6 receptor alpha chain than those that were MHCII negative (Figure 6B and C), and similar trends were observed for splenic DC. These data suggest that IL-6 has the ability to act directly on a subset of macrophages and activated dendritic cells during the acute challenge to *T. gondii*.

In order to directly test the effect of IL-6 on the production of IL-12 by accessory cells, purified splenic DC from WT or gp130 Y757F mice were cultured for 24 hours in the presence of LPS, or LPS and IFN- γ with or without IL-6. As shown in Figure 7D, WT DCs secreted IL-12p40 after stimulation with LPS and this response was enhanced in the presence of IFN- γ , but the addition of IL-6 to these cultures had no effect on IL-12 production. In contrast, DCs from gp130 Y757F mice produced equivalent levels of IL-12p40 in response to LPS alone, but when these cells were activated in the presence of LPS and IFN- γ (Figure 6D) there was a reduced IL-12p40 production compared to WT DCs, and the addition of IL-6 to these cultures almost completely blocked secretion of IL-12p40 (Figure 6D and E). Although WT and gp130 Y757F DCs produced equivalent levels of IL-6 (data not shown), the addition of anti-IL-6 blocking antibodies had no effect on the production of IL-12 by WT DCs (data not shown), but resulted in a significant increase in the production of IL-12p40 by gp130 Y757F DC (Figure 6E). Interestingly, when purified splenic DCs from gp130 Y757F mice were stimulated with LPS and IFN- γ in combination with IL-6, IL-11, IL-27 or Oncostatin M, only IL-6 had the capacity to block IL-12p40 production (Figure 6E).

Macrophages are also an innate source of IL-12 during toxoplasmosis (50, 51), and similar experiments were performed in order to assess if the production of IL-12 by these cells was also affected by IL-6. In response to LPS and IFN- γ WT bone marrow-derived macrophages (BMM Φ) produced more than 20 ng/mL of IL-12p40, and addition of IL-6 reduced the production of IL-12p40 by WT macrophages by approximately 25%, while blocking IL-6 during activation had no effect on IL-12p40 levels (Figure 6F). In contrast, LPS and IFN- γ activated macrophages from gp130 Y757F mice produce less IL-12p40 compared to WT controls the addition of exogenous IL-6 blocked the production of this cytokine by gp130 Y757F macrophages and blocking IL-6 during activation restored production of IL-12p40 to WT levels (Figure 6F). Moreover, the addition of other gp130-signaling cytokines had no effect on the production of IL-12p40 by gp130 Y757F macrophages (Figure 6F and G). Collectively, these data demonstrate that the observed defect in IL-12 production during toxoplasmosis in gp130 Y757F mice could be recapitulated *in vitro*, and that sustained signaling through gp130 by IL-6, but not other gp130-signaling cytokines, blocks pro-inflammatory responses by macrophages and DCs.

IL-6 blockade or addition of exogenous IL-12 restores protective immunity to *T. gondii* in gp130 Y757F mice

The data described above demonstrate that IL-6, but not other gp130-signaling cytokines, has an enhanced ability to directly block IL-12 production by gp130 Y757F APC and that approximately 50% of DCs and macrophages express both chains of the IL-6 receptor complex during infection (Figure 6A, B and C). Although infection of WT and gp130 Y757F mice results in similar levels of circulating IL-6 (~200–600 pg/mL), experiments were performed to assess the role of endogenous IL-6 in the susceptibility of gp130 Y757F mice to *T. gondii*. In these studies, gp130 Y757F mice were treated with anti-IL-6 blocking antibody or rat IgG and sacrificed at day 8 post-challenge in order to assess cytokine production, parasite burden and pathology. As expected, WT littermate controls survived the acute infection and effectively controlled parasite burden, while infected gp130 Y757F mice that received rat IgG were susceptible to challenge and had high parasite burdens (Figure 7A and B). In contrast, gp130 Y757F mice that were treated with anti-IL-6 survived the acute infection and had significantly lower parasite burdens than controls (Figure 7A and B). Consistent with our *in vitro* experiments, blocking IL-6 resulted in a significant increase in circulating levels of IL-12p40 and IFN- γ at day 3 (Figure 7C and D). In addition to significantly reducing parasite burdens in infected gp130 Y757F mice, anti-IL-6 treatment resulted in decreased infection-induced lung pathology (Figure 7E, F and G). Taken together, these studies demonstrate that, in the absence of SOCS3-mediated regulation of gp130-mediated signals, IL-6-signaling a key factor that antagonizes the initiation of protective immunity to *T. gondii*.

Though blockade of IL-6 during infection resulted in significantly decreased parasite burdens, the mechanism underlying these results remained unclear. Therefore, to address whether the capacity of IL-6 to block IL-12 production was the primary defect in the gp130 Y757F mice, these mice were treated with recombinant IL-12p70 for four days starting at the time of infection. Similar to the effects of IL-6 blockade, the administration of recombinant IL-12p70 to gp130 Y757F mice resulted in a significant reduction in parasite burden and these mice survived the acute infection (Figure 7A, B), associated with reduced infection-induced lung pathology (Figure 7E, F and H). The addition of exogenous IL-12p70 also restored IFN- γ to WT levels (Figure 7D), consistent with the idea that the early IFN- γ defect is a consequence of the reduced production of IL-12. Collectively, these results suggest that the ability of IL-6 to block IL-12 production in gp130 Y757F mice prevents the development of protective immunity to *T. gondii*.

Discussion

Previous studies have identified a critical role for IL-6 in resistance to *T. gondii* (24, 25), and although the mechanism by which IL-6 promotes resistance to this pathogen remains unclear, these findings are consistent with its role as a pro-inflammatory factor. Consequently, the finding in gp130 Y757F mice that IL-6 becomes a major inhibitor of IL-12 production was initially unexpected and there were several possible explanations for this observation. Recent studies have highlighted the importance of IL-6 and IL-27 signaling in promoting the generation of IL-10-producing CD4⁺ T cells that are essential for limiting infection-induced pathology (31, 40, 42–46, 52, 53). One scenario for the increased susceptibility of the gp130 Y757F mice was that enhanced gp130 signaling observed in T cells from gp130 Y757F mice explained the elevated IL-10 levels in these mice, which in turn antagonized the early production of IL-12. This hypothesis is consistent with previous work, which established that CD4⁺ T cells are the primary source of host-protective IL-10 during toxoplasmosis (46). However, the studies in which mutant T cells transferred into RAG mice were able to provide protection against *T. gondii* indicated that susceptibility of the gp130 Y757F mice was due to an innate defect that affected the production of IL-12.

IL-12 is an important factor that promotes NK and T cell expansion, differentiation and production of IFN- γ during numerous intracellular infections, including *T. gondii* (54). Although the IL-12 levels in gp130 Y757F mice eventually recover, previous studies have demonstrated that production of IL-12 during the first three days of infection is the most critical for host resistance (38, 50). Paradoxically, while the gp130 Y757F mice have an early defect in the production of IFN- γ by NK cells associated with lower levels of IL-12, at later time points there are normal numbers of IFN- γ ⁺ T cells. This compensatory response may be a consequence of the increased antigen load at later time points that leads to heightened T cell responses in gp130 Y757F mice. Alternatively, SOCS3 has been shown to negatively regulate the proliferation of activated T cells (55) and the inability of SOCS3 to limit gp130 signaling in mutant mice might result in increased proliferation of activated T cells. In support of this idea, both gp130 Y757F mice and gp130 Y759 mice, which have an analogous mutation, accumulate activated T cells with age (J Silver unpublished observations and (15))

Regardless of any intrinsic effects of the Y757F mutation on T cell function, our studies revealed that IL-6 was a potent inhibitor of IL-12 production by various macrophage and DC populations from these mice. In contrast, other gp130 family cytokines did not display this activity. Notably, IL-27 receptor alpha chain expression was not detected on APCs and we did not see any effects of IL-27 on the production of IL-12 or IL-10 by gp130 Y757F dendritic cells or macrophages. Nonetheless, the basis for this defect was initially unclear as the Y757F mutation prevents SOCS3 binding to gp130 but also abrogates SHP2/Erk signaling (56). However, gp130 Y757F and SOCS3 deficient cells (which have hyper SHP2/Erk signaling) have similar defects in the ability to produce IL-12 (48, 57), indicating that the inability to activate SHP2/Erk does not explain this phenotype. Rather, while SOCS3 normally abbreviates the duration of IL-6-mediated STAT3 activation, in its absence IL-6 generates a prolonged STAT3 signal, similar to that induced by IL-10, a potent antagonist of accessory cell inflammatory responses. Notably, when the Leptin and Erythropoietin receptors, which also activate STAT3, were engineered to yield sustained signaling profiles they also generated a similar anti-inflammatory outcome (57). Thus, the studies presented here indicate that in the gp130 Y757F mice challenged with *T. gondii* the IL-6 that is produced becomes an efficient antagonist of IL-12 production that is essential to control this parasite.

The observation that IL-6 drives the hematopoietic defects observed in aged gp130 Y757F mice (10, 10–13), indicates that IL-6 signaling impacts acts globally on an array of cell populations in these mice. Expression of gp130 cytokine family-specific receptor alpha chains is one mechanism that ensures appropriate cell- and tissue-specific responses to gp130 cytokines, and the finding that significant populations of macrophages and DCs did not express the IL-6 receptor alpha suggested that IL-6 does not influence these cells. However, the ability of this cytokine to bind to a soluble IL-6 receptor alpha chain enables any cell expressing gp130 to respond to IL-6 (58). This process of trans signaling has been shown to affect multiple cell populations and preliminary experiments treating gp130 Y757F mice with a soluble gp130 receptor Fc, which is specifically designed to block IL-6 trans-signaling, reverses the susceptibility of gp130 Y757F mice to toxoplasmosis (unpublished observations). Thus, it appears that trans-signaling provides a significant contribution to the IL-6-mediated susceptibility to *T. gondii* in these mutant mice.

Although IL-6 is traditionally described as a pro-inflammatory cytokine, it is important to recognize that even in WT macrophages (but not DC) we observed a modest but reproducible inhibitory effect of IL-6 on the production of IL-12p40. Thus, although the anti-inflammatory effects of IL-6 are exaggerated in the absence of appropriate regulation by SOCS3 (this study and (48, 57)), this inhibitory effect may represent a physiological

function of IL-6. Consistent with this hypothesis, previous work has shown that IL-6 can antagonize IL-12 production by pulmonary DCs(59), block T_H1 differentiation and antagonize the anti-microbial activities of macrophages (60–63). Furthermore, IL-6 deficient mice over-produce several pro-inflammatory cytokines after local or systemic endotoxemia (64). One implication of these studies is that while IL-6 is constitutively produced during many types of acute and chronic inflammation its function may change depending on context. Thus, the type of abbreviated signals generated following initial exposure to IL-6 may promote acute inflammatory responses, but prolonged and repeated exposure to IL-6, even in the presence of SOCS3, might be expected to provide a profile of sustained STAT3 activity accompanied by an inhibitory effect. In other words, there is evidence that IL-6 is part of a regulatory loop that is important to initiate inflammation, but can also act to limit this response in a chronic setting. This is a concept that, to the best of our knowledge, has yet to be directly tested, but is especially relevant in the context of the development of treatments designed to block IL-6 or STAT3 in chronic inflammatory disorders (18, 65). Regardless, the studies presented here highlight the need to appropriately control the signals provided by IL-6 during infection, and demonstrate the profound impact that alterations in gp130 signaling can have on the generation of protective immunity to an opportunistic pathogen.

Supplementary Material

Refer to Web version on PubMed Central for supplementary material.

Acknowledgments

Ludwig Institute, State of Pennsylvania, National Institutes of Health Grant Number AI42334, National Institutes of Health Grant Number AI 084882, Jonathan Silver is supported by T32 training grant number AI007532, State of Pennsylvania and the Penn Center for Molecular Studies in Digestive and Liver Diseases.

Bibliography

1. Taga T, Kishimoto T. Gp130 and the interleukin-6 family of cytokines. *Annu Rev Immunol.* 1997; 15:797–819. [PubMed: 9143707]
2. O'Shea JJ, Gadina M, Schreiber RD. Cytokine signaling in 2002: new surprises in the Jak/Stat pathway. *Cell.* 2002; 109(Suppl):S121–31. [PubMed: 11983158]
3. O'Shea JJ, Murray PJ. Cytokine signaling modules in inflammatory responses. *Immunity.* 2008; 28:477–487. [PubMed: 18400190]
4. De Souza D, Fabri LJ, Nash A, Hilton DJ, Nicola NA, Baca M. SH2 domains from suppressor of cytokine signaling-3 and protein tyrosine phosphatase SHP-2 have similar binding specificities. *Biochemistry.* 2002; 41:9229–9236. [PubMed: 12119038]
5. Nicholson SE, De Souza D, Fabri LJ, Corbin J, Willson TA, Zhang JG, Silva A, Asimakis M, Farley A, Nash AD, Metcalf D, Hilton DJ, Nicola NA, Baca M. Suppressor of cytokine signaling-3 preferentially binds to the SHP-2-binding site on the shared cytokine receptor subunit gp130. *Proc Natl Acad Sci U S A.* 2000; 97:6493–6498. [PubMed: 10829066]
6. Schmitz J, Weissenbach M, Haan S, Heinrich PC, Schaper F. SOCS3 exerts its inhibitory function on interleukin-6 signal transduction through the SHP2 recruitment site of gp130. *J Biol Chem.* 2000; 275:12848–12856. [PubMed: 10777583]
7. Babon JJ, Sabo JK, Soetopo A, Yao S, Bailey MF, Zhang JG, Nicola NA, Norton RS. The SOCS box domain of SOCS3: structure and interaction with the elongin BC-cullin5 ubiquitin ligase. *J Mol Biol.* 2008; 381:928–940. [PubMed: 18590740]
8. Tebbutt NC, Giraud AS, Inglese M, Jenkins B, Waring P, Clay FJ, Malki S, Alderman BM, Grail D, Hollande F, Heath JK, Ernst M. Reciprocal regulation of gastrointestinal homeostasis by SHP2 and STAT-mediated trefoil gene activation in gp130 mutant mice. *Nat Med.* 2002; 8:1089–1097. [PubMed: 12219085]

9. Ohtani T, Ishihara K, Atsumi T, Nishida K, Kaneko Y, Miyata T, Itoh S, Narimatsu M, Maeda H, Fukada T, Itoh M, Okano H, Hibi M, Hirano T. Dissection of signaling cascades through gp130 in vivo: reciprocal roles for STAT3- and SHP2-mediated signals in immune responses. *Immunity*. 2000; 12:95–105. [PubMed: 10661409]
10. Jenkins BJ, Roberts AW, Greenhill CJ, Najdovska M, Lundgren-May T, Robb L, Grail D, Ernst M. Pathologic consequences of STAT3 hyperactivation by IL-6 and IL-11 during hematopoiesis and lymphopoiesis. *Blood*. 2007; 109:2380–2388. [PubMed: 17082315]
11. Jenkins BJ, Grail D, Nheu T, Najdovska M, Wang B, Waring P, Inglese M, McLoughlin RM, Jones SA, Topley N, Baumann H, Judd LM, Giraud AS, Boussioutas A, Zhu HJ, Ernst M. Hyperactivation of Stat3 in gp130 mutant mice promotes gastric hyperproliferation and desensitizes TGF-beta signaling. *Nat Med*. 2005; 11:845–52. [PubMed: 16041381]
12. Jenkins BJ, Roberts AW, Najdovska M, Grail D, Ernst M. The threshold of gp130-dependent STAT3 signaling is critical for normal regulation of hematopoiesis. *Blood*. 2005; 105:3512–3520. [PubMed: 15650055]
13. Ernst M, Najdovska M, Grail D, Lundgren-May T, Buchert M, Tye H, Matthews VB, Armes J, Bhathal PS, Hughes NR, Marcussen EG, Karras JG, Na S, Sedgwick JD, Hertzog PJ, Jenkins BJ. STAT3 and STAT1 mediate IL-11-dependent and inflammation-associated gastric tumorigenesis in gp130 receptor mutant mice. *J Clin Invest*. 2008; 118:1727–1738. [PubMed: 18431520]
14. Atsumi T, Ishihara K, Kamimura D, Ikushima H, Ohtani T, Hirota S, Kobayashi H, Park SJ, Saeki Y, Kitamura Y, Hirano T. A point mutation of Tyr-759 in interleukin 6 family cytokine receptor subunit gp130 causes autoimmune arthritis. *J Exp Med*. 2002; 196:979–990. [PubMed: 12370259]
15. Sawa S, Kamimura D, Jin GH, Morikawa H, Kamon H, Nishihara M, Ishihara K, Murakami M, Hirano T. Autoimmune arthritis associated with mutated interleukin (IL)-6 receptor gp130 is driven by STAT3/IL-7-dependent homeostatic proliferation of CD4+ T cells. *J Exp Med*. 2006; 203:1459–1470. [PubMed: 16717113]
16. Rebouissou S, Amessou M, Couchy G, Poussin K, Imbeaud S, Pilati C, Iazard T, Balabaud C, Bioulac-Sage P, Zucman-Rossi J. Frequent in-frame somatic deletions activate gp130 in inflammatory hepatocellular tumours. *Nature*. 2009; 457:200–204. [PubMed: 19020503]
17. Nowell MA, Williams AS, Carty SA, Scheller J, Hayes AJ, Jones GW, Richards PJ, Slinn S, Ernst M, Jenkins BJ, Topley N, Rose-John S, Jones SA. Therapeutic targeting of IL-6 trans signaling counteracts STAT3 control of experimental inflammatory arthritis. *J Immunol*. 2009; 182:613–622. [PubMed: 19109195]
18. Nishimoto N, Yoshizaki K, Miyasaka N, Yamamoto K, Kawai S, Takeuchi T, Hashimoto J, Azuma J, Kishimoto T. Treatment of rheumatoid arthritis with humanized anti-interleukin-6 receptor antibody: a multicenter, double-blind, placebo-controlled trial. *Arthritis Rheum*. 2004; 50:1761–1769. [PubMed: 15188351]
19. Hunter CA, Remington JS. Immunopathogenesis of toxoplasmic encephalitis. *J Infect Dis*. 1994; 170:1057–1067. [PubMed: 7963693]
20. Sher A, Denkers EY, Gazzinelli RT. Induction and regulation of host cell-mediated immunity by *Toxoplasma gondii*. *Ciba found Symp*. 1995; 195:95–104. discussion 104–9. [PubMed: 8724832]
21. Sher A, Collazzo C, Scanga C, Jankovic D, Yap G, Aliberti J. Induction and regulation of IL-12-dependent host resistance to *Toxoplasma gondii*. *Immunol Res*. 2003; 27:521–528. [PubMed: 12857995]
22. Denkers EY, Gazzinelli RT. Regulation and function of T-cell-mediated immunity during *Toxoplasma gondii* infection. *Clin Microbiol Rev*. 1998; 11:569–588. [PubMed: 9767056]
23. Suzuki Y, Conley FK, Remington JS. Importance of endogenous IFN-gamma for prevention of toxoplasmic encephalitis in mice. *J Immunol*. 1989; 143:2045–2050. [PubMed: 2506275]
24. Suzuki Y, Rani S, Liesenfeld O, Kojima T, Lim S, Nguyen TA, Dalrymple SA, Murray R, Remington JS. Impaired resistance to the development of toxoplasmic encephalitis in interleukin-6-deficient mice. *Infect Immun*. 1997; 65:2339–2345. [PubMed: 9169772]
25. Jebbari H, Roberts CW, Ferguson DJ, Bluethmann H, Alexander J. A protective role for IL-6 during early infection with *Toxoplasma gondii*. *Parasite Immunol*. 1998; 20:231–239. [PubMed: 9651924]

26. Drogemuller K, Helmuth U, Brunn A, Sakowicz-Burkiewicz M, Gutmann DH, Mueller W, Deckert M, Schluter D. Astrocyte gp130 expression is critical for the control of *Toxoplasma* encephalitis. *J Immunol.* 2008; 181:2683–2693. [PubMed: 18684959]
27. Villarino A, Hibbert L, Lieberman L, Wilson E, Mak T, Yoshida H, Kastelein RA, Saris C, Hunter CA. The IL-27R (WSX-1) is required to suppress T cell hyperactivity during infection. *Immunity.* 2003; 19:645–655. [PubMed: 14614852]
28. Stumhofer JS, Laurence A, Wilson EH, Huang E, Tato CM, Johnson LM, Villarino AV, Huang Q, Yoshimura A, Sehy D, Saris CJ, O’Shea JJ, Hennighausen L, Ernst M, Hunter CA. Interleukin 27 negatively regulates the development of interleukin 17-producing T helper cells during chronic inflammation of the central nervous system. *Nat Immunol.* 2006; 7:937–945. [PubMed: 16906166]
29. Silver JS, Hunter CA. Gp130 at the Nexus of Inflammation, Autoimmunity, and Cancer. *J Leukoc Biol.* 2010
30. Wilson EH, Wille-Reece U, Dzierszynski F, Hunter CA. A critical role for IL-10 in limiting inflammation during toxoplasmic encephalitis. *J Neuroimmunol.* 2005; 165:63–74. [PubMed: 16005735]
31. Stumhofer JS, Silver JS, Laurence A, Porrett PM, Harris TH, Turka LA, Ernst M, Saris CJ, O’Shea JJ, Hunter CA. Interleukins 27 and 6 induce STAT3-mediated T cell production of interleukin 10. *Nat Immunol.* 2007; 8:1363–1371. [PubMed: 17994025]
32. Taylor GA, Feng CG, Sher A. p47 GTPases: regulators of immunity to intracellular pathogens. *Nat Rev Immunol.* 2004; 4:100–109. [PubMed: 15040583]
33. Collazo CM, Yap GS, Sempowski GD, Lusby KC, Tessarollo L, Woude GF, Sher A, Taylor GA. Inactivation of LRG-47 and IRG-47 reveals a family of interferon gamma-inducible genes with essential, pathogen-specific roles in resistance to infection. *J Exp Med.* 2001; 194:181–188. [PubMed: 11457893]
34. Taylor GA, Collazo CM, Yap GS, Nguyen K, Gregorio TA, Taylor LS, Eagleson B, Secret L, Southon EA, Reid SW, Tessarollo L, Bray M, McVicar DW, Komschlies KL, Young HA, Biron CA, Sher A, Vande Woude GF. Pathogen-specific loss of host resistance in mice lacking the IFN-gamma-inducible gene IGTP. *Proc Natl Acad Sci U S A.* 2000; 97:751–755. [PubMed: 10639151]
35. Denkers EY, Gazzinelli RT, Martin D, Sher A. Emergence of NK1.1+ cells as effectors of IFN-gamma dependent immunity to *Toxoplasma gondii* in MHC class I-deficient mice. *J Exp Med.* 1993; 178:1465–1472. [PubMed: 8228800]
36. Hunter CA, Subauste CS, Van Cleave VH, Remington JS. Production of gamma interferon by natural killer cells from *Toxoplasma gondii*-infected SCID mice: regulation by interleukin-10, interleukin-12, and tumor necrosis factor alpha. *Infect Immun.* 1994; 62:2818–2824. [PubMed: 7911785]
37. Passos ST, Silver JS, O’Hara AC, Sehy D, Stumhofer JS, Hunter CA. IL-6 promotes NK cell production of IL-17 during toxoplasmosis. *J Immunol.* 2010; 184:1776–1783. [PubMed: 20083665]
38. Khan IA, Matsuura T, Kasper LH. Interleukin-12 enhances murine survival against acute toxoplasmosis. *Infect Immun.* 1994; 62:1639–1642. [PubMed: 7909536]
39. Sher A, Oswald IP, Hieny S, Gazzinelli RT. *Toxoplasma gondii* induces a T-independent IFN-gamma response in natural killer cells that requires both adherent accessory cells and tumor necrosis factor-alpha. *J Immunol.* 1993; 150:3982–3989. [PubMed: 8473745]
40. Gazzinelli RT, Wysocka M, Hieny S, Scharon-Kersten T, Cheever A, Kuhn R, Muller W, Trinchieri G, Sher A. In the absence of endogenous IL-10, mice acutely infected with *Toxoplasma gondii* succumb to a lethal immune response dependent on CD4+ T cells and accompanied by overproduction of IL-12, IFN-gamma and TNF-alpha. *J Immunol.* 1996; 157:798–805. [PubMed: 8752931]
41. D’Andrea A, Aste-Amezaga M, Valiante NM, Ma X, Kubin M, Trinchieri G. Interleukin 10 (IL-10) inhibits human lymphocyte interferon gamma-production by suppressing natural killer cell stimulatory factor/IL-12 synthesis in accessory cells. *J Exp Med.* 1993; 178:1041–1048. [PubMed: 8102388]

42. Awasthi A, Carrier Y, Peron JP, Bettelli E, Kamanaka M, Flavell RA, Kuchroo VK, Oukka M, Weiner HL. A dominant function for interleukin 27 in generating interleukin 10-producing anti-inflammatory T cells. *Nat Immunol.* 2007; 8:1380–1389. [PubMed: 17994022]
43. Fitzgerald DC, Zhang GX, El-Behi M, Fonseca-Kelly Z, Li H, Yu S, Saris CJ, Gran B, Ciric B, Rostami A. Suppression of autoimmune inflammation of the central nervous system by interleukin 10 secreted by interleukin 27-stimulated T cells. *Nat Immunol.* 2007; 8:1372–1379. [PubMed: 17994023]
44. McGeachy MJ, Bak-Jensen KS, Chen Y, Tato CM, Blumenschein W, McClanahan T, Cua DJ. TGF-beta and IL-6 drive the production of IL-17 and IL-10 by T cells and restrain T(H)-17 cell-mediated pathology. *Nat Immunol.* 2007; 8:1390–1397. [PubMed: 17994024]
45. Anderson CF, Stumhofer JS, Hunter CA, Sacks D. IL-27 regulates IL-10 and IL-17 from CD4+ cells in nonhealing *Leishmania major* infection. *J Immunol.* 2009; 183:4619–4627. [PubMed: 19748991]
46. Jankovic D, Kullberg MC, Feng CG, Goldszmid RS, Collazo CM, Wilson M, Wynn TA, Kamanaka M, Flavell RA, Sher A. Conventional T-bet(+)Foxp3(-) Th1 cells are the major source of host-protective regulatory IL-10 during intracellular protozoan infection. *J Exp Med.* 2007; 204:273–283. [PubMed: 17283209]
47. Croker BA, Krebs DL, Zhang JG, Wormald S, Willson TA, Stanley EG, Robb L, Greenhalgh CJ, Forster I, Clausen BE, Nicola NA, Metcalf D, Hilton DJ, Roberts AW, Alexander WS. SOCS3 negatively regulates IL-6 signaling in vivo. *Nat Immunol.* 2003; 4:540–545. [PubMed: 12754505]
48. Yasukawa H, Ohishi M, Mori H, Murakami M, Chinen T, Aki D, Hanada T, Takeda K, Akira S, Hoshijima M, Hirano T, Chien KR, Yoshimura A. IL-6 induces an anti-inflammatory response in the absence of SOCS3 in macrophages. *Nat Immunol.* 2003; 4:551–556. [PubMed: 12754507]
49. Lang R, Pauleau AL, Parganas E, Takahashi Y, Mages J, Ihle JN, Rutschman R, Murray PJ. SOCS3 regulates the plasticity of gp130 signaling. *Nat Immunol.* 2003; 4:546–550. [PubMed: 12754506]
50. Gazzinelli RT, Hieny S, Wynn TA, Wolf S, Sher A. Interleukin 12 is required for the T-lymphocyte-independent induction of interferon gamma by an intracellular parasite and induces resistance in T-cell-deficient hosts. *Proc Natl Acad Sci U S A.* 1993; 90:6115–6119. [PubMed: 8100999]
51. Middleton MK, Zukas AM, Rubinstein T, Kinder M, Wilson EH, Zhu P, Blair IA, Hunter CA, Pure E. 12/15-Lipoxygenase-Dependent Myeloid Production of Interleukin-12 is Essential for Resistance to Chronic Toxoplasmosis. *Infect Immun.* 2009; 77:5690–5700. [PubMed: 19822654]
52. Saraiva M, O'Garra A. The regulation of IL-10 production by immune cells. *Nat Rev Immunol.* 2010; 10:170–181. [PubMed: 20154735]
53. Stumhofer JS, Hunter CA. Advances in understanding the anti-inflammatory properties of IL-27. *Immunol Lett.* 2008; 117:123–130. [PubMed: 18378322]
54. Trinchieri G. Interleukin-12 and the regulation of innate resistance and adaptive immunity. *Nature Reviews Immunology.* 2003; 3:133–146.
55. Yu CR, Mahdi RM, Ebong S, Vistica BP, Gery I, Egwuagu CE. Suppressor of cytokine signaling 3 regulates proliferation and activation of T-helper cells. *J Biol Chem.* 2003; 278:29752–29759. [PubMed: 12783879]
56. Ernst M, Jenkins BJ. Acquiring signalling specificity from the cytokine receptor gp130. *Trends Genet.* 2004; 20:23–32. [PubMed: 14698616]
57. El Kasmi KC, Holst J, Coffre M, Mielke L, de Pauw A, Lhocine N, Smith AM, Rutschman R, Kaushal D, Shen Y, Suda T, Donnelly RP, Myers MG Jr, Alexander W, Vignali DA, Watowich SS, Ernst M, Hilton DJ, Murray PJ. General nature of the STAT3-activated anti-inflammatory response. *J Immunol.* 2006; 177:7880–7888. [PubMed: 17114459]
58. Rose-John S, Scheller J, Elson G, Jones SA. Interleukin-6 biology is coordinated by membrane-bound and soluble receptors: role in inflammation and cancer. *J Leukoc Biol.* 2006; 80:227–236. [PubMed: 16707558]
59. Dodge IL, Carr MW, Cernadas M, Brenner MB. IL-6 production by pulmonary dendritic cells impedes Th1 immune responses. *J Immunol.* 2003; 170:4457–4464. [PubMed: 12707321]

60. Beaman MH, Hunter CA, Remington JS. Enhancement of intracellular replication of *Toxoplasma gondii* by IL-6. Interactions with IFN-gamma and TNF-alpha. *J Immunol.* 1994; 153:4583–4587. [PubMed: 7963530]
61. Diehl S, Anguita J, Hoffmeyer A, Zapton T, Ihle JN, Fikrig E, Rincon M. Inhibition of Th1 differentiation by IL-6 is mediated by SOCS1. *Immunity.* 2000; 13:805–815. [PubMed: 11163196]
62. Nagabhushanam V, Solache A, Ting LM, Escaron CJ, Zhang JY, Ernst JD. Innate inhibition of adaptive immunity: *Mycobacterium tuberculosis*-induced IL-6 inhibits macrophage responses to IFN-gamma. *J Immunol.* 2003; 171:4750–4757. [PubMed: 14568951]
63. Bermudez LE, Wu M, Petrofsky M, Young LS. Interleukin-6 antagonizes tumor necrosis factor-mediated mycobacteriostatic and mycobactericidal activities in macrophages. *Infect Immun.* 1992; 60:4245–4252. [PubMed: 1328056]
64. Xing Z, Gauldie J, Cox G, Baumann H, Jordana M, Lei XF, Achong MK. IL-6 is an antiinflammatory cytokine required for controlling local or systemic acute inflammatory responses. *J Clin Invest.* 1998; 101:311–320. [PubMed: 9435302]
65. Grivennikov SI, Greten FR, Karin M. Immunity, Inflammation, and Cancer. *Cell.* 2010; 140:883–899. [PubMed: 20303878]

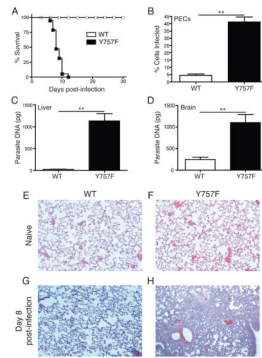


Figure 1.

Gp130 Y757F mice are susceptible to infection with *Toxoplasma gondii*. **A)** Survival of WT (n=15) and gp130 Y757F mice (n=12) infected intraperitoneally with 20 cysts of the Me49 strain of *T. gondii*. **B)** Percentage of *T. gondii*-infected peritoneal exudate cells (PECs) at day 8 post infection in WT (n=14) and gp130 Y757F (n=12) mice. **p<.001. Enumeration of parasite DNA by real-time PCR in livers (**C**) and brains (**D**) of infected WT (n=10) and gp130 Y757F (n=14) mice at day 8 post-infection. **p<.001. Histopathology of lungs from naïve and infected WT (**E and G**) and gp130 Y757F (**F and H**) mice, analyzed by staining with hematoxylin and eosin at day 8 post-infection.

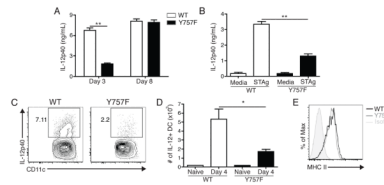
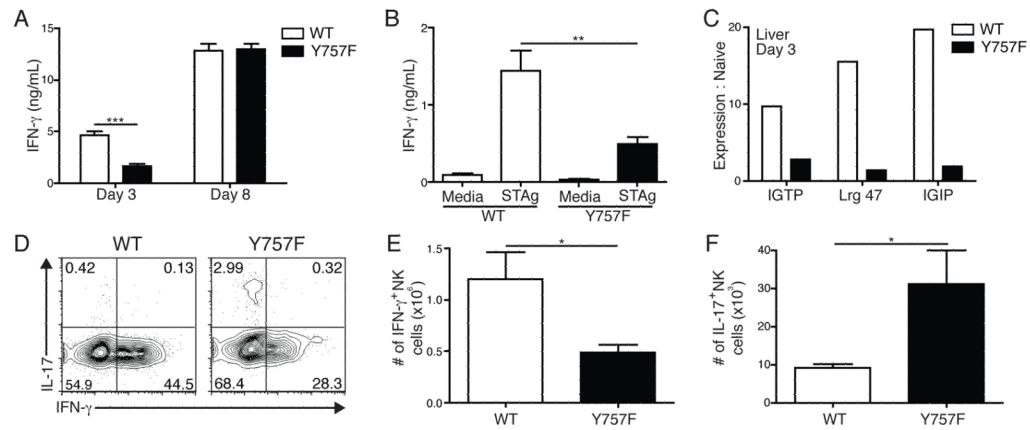


Figure 2.

Gp130 Y757F mice have an early defect in the ability to produce IL-12 during infection with *T. gondii*. **A)** Kinetics of IL-12p40 production in the serum of infected WT (n=8) or gp130 Y757F mice (n=10), as measured by ELISA. **p<.001. **B)** ELISA of IFN-g levels in the supernatants of splenocytes isolated from WT and gp130 Y757F mice that were incubated with STAg for 48 hours. Data are representative of three independent experiments. **p<.001. **C)** Flow cytometry of intracellular IL-12p40 in DC isolated from PECs of infected WT or gp130 Y757F mice at day 4 post-infection; cells were incubated with BFA for 6 hours before staining. **D)** Total number of IL-12+ DC in the PECs at day 4 post-infection in WT or gp130 Y757F mice, calculated from percentages based on flow cytometry. *p<.01 **E)** Representative histogram of MHC II expression on DC from the PEC of WT (solid line) or gp130 Y757F (dotted line) mice at day 4 post-infection. Data are representative of two independent experiments.

**Figure 3.**

Gp130 Y757F mice have lower levels of IFN- γ early after *T. gondii* infection. **A)** Kinetics of IFN- γ production in the serum of infected WT (n=10) or gp130 Y757F mice (n=11), as measured by ELISA. Data are pooled from 4 independent experiments, ***p<.001. **B)** At day 3 post-infection, whole splenocytes from WT and Y757F mice were stimulated with STAg for 48 hours and assayed for IFN- γ . Data are representative of 4 independent experiments. **p<.01. **C)** Real time PCR of total cellular RNA isolated from the livers of WT and Y757F mice at day 3 post-infection to detect IGTP, Lrg 47 and IGIP mRNA. Data are representative of two independent experiments. **D)** Flow cytometry of IL-17A vs. IFN- γ from splenocytes isolated from WT or gp130 Y757F mice at day 4 post-infection. Plots are gated on NK1.1+ CD3- cells; cells were incubated with PMA, Ionomycin and BFA for 4 hours before being stained. Total numbers of IFN- γ + (**E)** and IL-17+ (**F)** splenic NK cells from WT (n=5) and Y757F mice (n=7) at day 4 post-infection. Data are pooled from two independent experiments. *p<.05.

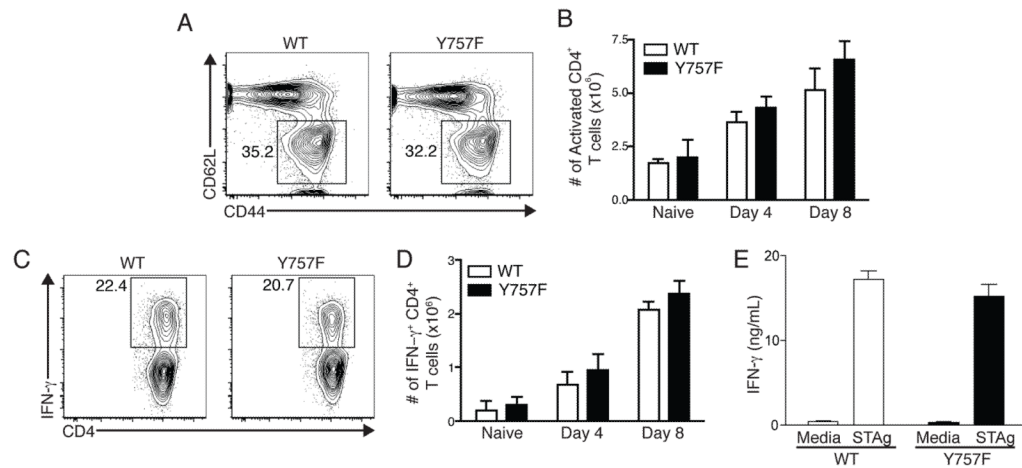


Figure 4.

Infection-induced T cell activation is normal in Y757F mice. **A)** Flow cytometry of splenocytes from WT or gp130 Y757F mice at day 8 post-infection showing expression of CD62L and CD44. Gated on CD3⁺ CD4⁺ cells. **B)** The number of CD44^{hi} CD62L^{low} CD4⁺ T cells was enumerated in naïve WT and gp130 Y757F mice, and at day 4 and day 8 post-infection. $n \geq 5$ mice per time point. **C)** Flow cytometry of IFN- γ in splenocytes isolated from WT or gp130 Y757F mice at day 8 post-infection. Gated on CD3⁺ CD4⁺ events; cells were incubated with PMA, Ionomycin and BFA for 4 hours before being stained. **D)** Enumeration of IFN- γ ⁺ CD4⁺ T cells in naïve or infected WT or gp130 Y757F mice. $n \geq 5$ mice per time point. **E)** ELISA of IFN- γ levels from cultures of splenocytes isolated at day 8 post-infection and incubated with STAg for 48 hours. Data are representative of 4 independent experiments.

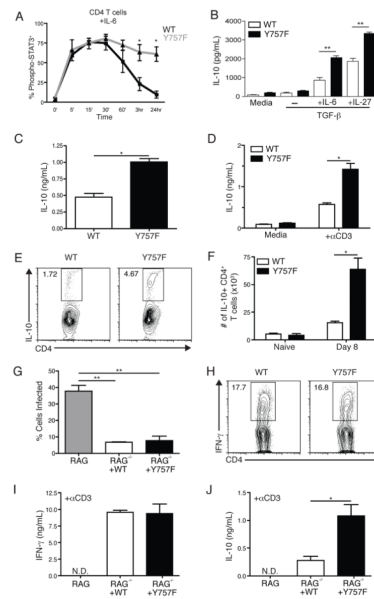


Figure 5.

Gp130 Y757F T cells produce augmented levels of IL-10 in response to IL-6 and IL-27. Purified CD4⁺ T cells from naïve WT and Y757F mice were stimulated *in vitro* with IL-6 (A) for various time points before being fixed, permeabilized and stained for intracellular phosphorylated STAT3. Data are pooled from 5 independent experiments. **p*<.01. B) Purified CD4⁺ T cells from naïve WT or gp130 Y757F mice were activated with anti-CD3 and anti-CD28 for 48 hours in the presence of TGF-β with IL-6 or IL-27. IL-10 levels in culture supernatants were determined by ELISA. Data are representative of 4 independent experiments with similar results. ***p*<.001. C) IL-10 levels in the serum of infected WT (5) or gp130 Y757F (8) mice were determined by ELISA at day 8 post-infection. **p*<.01. Data are pooled from two independent experiments. D) At day 8 post-infection, whole splenocytes from WT and Y757F mice were stimulated with media or anti-CD3 for 48 hours and assayed for IL-10 by ELISA. Data are representative of three independent experiments. **p*<.01. E) Flow cytometry of IL-10 from splenocytes isolated from WT or gp130 Y757F mice at day 8 post-infection. Gated on CD3⁺ CD4⁺ events, cells were incubated with PMA, Ionomycin and BFA for 4 hours before being stained. F) The total number of IL-10⁺ CD4⁺ T cells was calculated in WT (n=5) and Y757F mice (n=6) at 8 days post-infection. Data are pooled from two independent experiments. **p*<.01. G) 10 million splenic CD4⁺ and CD8⁺ T cells were isolated from WT and Y757F mice and transferred into RAG KO mice. The recipient RAG mice that received T cells from WT (n=5) or gp130 Y757F mice (n=5) were infected with *T. gondii* and at 8 days post-infection the percentage of infected PECs was enumerated. ***p*<.001. H) Flow cytometry of IFN-γ from splenocytes isolated from RAG KO mice that received WT or gp130 Y757F mice at day 8 post-infection. Gated on CD3⁺ CD4⁺ events; cells were incubated with PMA, Ionomycin and BFA for 4 hours before being stained. I) At 8 days post-infection, whole splenocytes from recipient RAG KO mice were stimulated with anti-CD3 for 48 hours and assayed for IFN-γ by ELISA. J) At 8 days post-infection, whole splenocytes from recipient RAG KO mice were stimulated with anti-CD3 for 48 hours and assayed for IL-10 by ELISA. Data are representative of 3 independent experiments with similar results. **p*<.01.

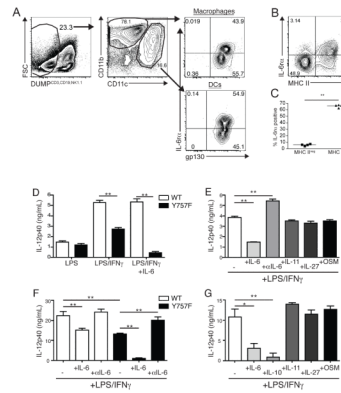


Figure 6.

IL-6 blocks the production of IL-12 by gp130 Y757F APC. **A)** Flow cytometry of IL-6 receptor alpha and gp130 expression on PECs from WT mice at day 4 post-infection. Gated on CD3/CD19/NK1.1^{neg}, CD11c or CD11b⁺ cells. Representative FACS plot (**B**) and enumeration (**C**) of the percentage of MHC II negative or MHC II positive DCs that express the IL-6 receptor alpha. Data are representative of two independent experiments with similar results. **D)** Purified splenic DC from naïve WT and Y757F mice were stimulated *in vitro* with LPS, IFN- γ and IL-6 for 24 hours before IL-12p40 was measured in culture supernatants by ELISA. **E)** Purified splenic DC from naïve gp130 Y757F mice were stimulated *in vitro* with LPS, IFN- γ and IL-6, IL-11, IL-27, Oncostatin M or anti-IL-6 antibodies for 24 hours before IL-12p40 was measured in culture supernatants by ELISA. N=3 samples per condition. Data are representative of 3 independent experiments. **F)** Bone marrow-derived macrophages from WT and Y757F mice were stimulated *in vitro* with LPS, IFN- γ and IL-6 or anti-IL-6 antibodies for 24 hours before IL-12p40 was measured in culture supernatants by ELISA. **G)** Bone marrow-derived macrophages from gp130 Y757F mice were stimulated *in vitro* with LPS, IFN- γ and IL-6, IL-10, IL-11, IL-27 or Oncostatin M for 24 hours before IL-12p40 was measured in culture supernatants by ELISA.

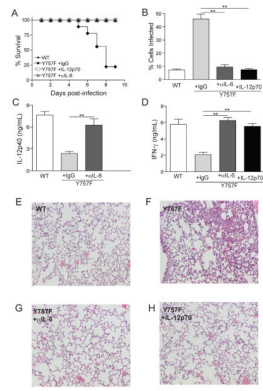


Figure 7.

Anti-IL-6 treatment, or administration of IL-12p70, rescues gp130 Y757F mice. **A)** Survival of *T. gondii*-infected WT (n=5) or gp130 Y757F mice that were treated with Rat IgG (n=12), anti-IL-6 antibodies (n=9) or recombinant IL-12p70 (n=6). **B)** Percentage of PECs infected in WT (n=5) or gp130 Y757F mice that were treated with Rat IgG (n=5), anti-IL-6 antibodies (n=8) or recombinant IL-12p70 (n=5). **C)** At day 3 post-infection, WT (n=5) or gp130 Y757F mice treated with Rat IgG (n=7) or anti-IL-6 blocking antibodies (n=8) were bled and the levels of circulating IL-12p40 was determined by ELISA. **p<.01. **D)** At day 3 post-infection, WT (n=5) or gp130 Y757F mice treated with Rat IgG (n=7), anti-IL-6 blocking antibodies (n=8), or recombinant IL-12p70 (n=5) were bled and the levels of circulating IFN-γ was determined by ELISA. **p<.01. **E-H)** Histopathology of lungs from infected WT or gp130 Y757F mouse that was treated with Rat IgG, anti-IL-6 or recombinant IL-12p70 and stained with hemotoxylin and eosin.